

Dendritic Surface Functionalization of Biodegradable Polymer Assemblies

ALI NAZEMI,¹ RYAN C. AMOS,² COLIN V. BONDUELLE,¹ ELIZABETH R. GILLIES^{1,3}

¹Department of Chemistry, The University of Western Ontario, 1151 Richmond St., London, Canada N6A 5B7

²Biomedical Engineering Graduate Program, The University of Western Ontario, 1151 Richmond St., London, Canada N6A 5B9

³Department of Chemical and Biochemical Engineering, The University of Western Ontario, 1151 Richmond St., London, Canada N6A 5B9

Received 8 February 2011; accepted 23 March 2011

DOI: 10.1002/pola.24686

Published online 14 April 2011 in Wiley Online Library (wileyonlinelibrary.com).

ABSTRACT: The functionalization of nanomaterials with dendritic surface moieties was recently demonstrated to be an effective means of displaying biological ligands and potentially modulating the biological properties of these materials. With the aim of extending this surface functionalization approach to biodegradable polymer assemblies, poly(ethylene oxide)-polycaprolactone (PEO-PCL) block copolymers with terminal azide or methoxy groups were prepared and were assembled to form micelles or vesicles with varying loadings of surface azides. Dendrons bearing peripheral amines, guanidines, or hydroxyls were prepared and conjugated to the assemblies, and the conjugation yields were measured and compared as a function of azide loading and assembly type (micelle versus vesicle). A small molecule rhodamine derivative was also con-

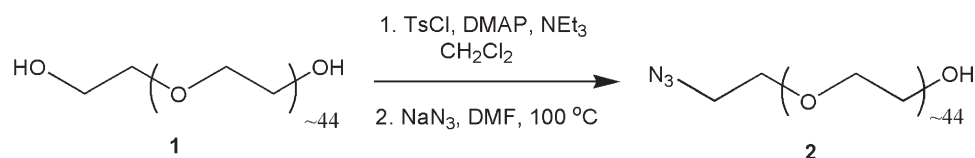
jugated, allowing the effect of sterics to be studied. The effects of the surface functionalization on the aggregation state of the assemblies were studied by light scattering and transmission electron microscopy. Overall, the results revealed interesting differences between the two systems with respect to both the reaction yields and the stabilities. Furthermore, micelles functionalized with dendrons bearing peripheral guanidines were found to exhibit enhanced cell uptake relative to control micelles, demonstrating that this approach can be used to modulate the biological properties of the materials. © 2011 Wiley Periodicals, Inc. *J Polym Sci Part A: Polym Chem* 49: 2546–2559, 2011

KEYWORDS: biodegradable; block copolymers; dendrimers; micelles; vesicles

INTRODUCTION In solution, amphiphilic block copolymers can undergo self-assembly, forming a diverse range of structures from spherical micelles¹ to helical rods,² toroids,³ vesicles,^{4,5} tubes,⁶ and multicompartiment cylinders.⁷ In recent years, micelles and vesicles have received significant attention as they can be readily accessed using a wide range of block copolymers by controlling the relative volume fractions of the constituent blocks.⁸ Relative to their counterparts formed from low molecular weight (MW) surfactants,⁹ these assemblies typically exhibit much lower critical aggregation concentrations and enhanced thermodynamic and kinetic stabilities.^{7,10} Because of these properties, there has been particular interest in biomedical applications of these materials, and they have been demonstrated as promising carriers of proteins,^{11–13} hydrophilic and hydrophobic drugs,^{14–17} and imaging contrast agents.^{18–20} Micelles and vesicles are complementary systems in that micelles possess a hydrophobic core that is typically used to encapsulate hydrophobic species, whereas vesicles possess an aqueous core capable of encapsulating water soluble species. However, vesicles also possess a hydrophobic membrane that can also encapsulate hydrophobes, making these assemblies multifunctional.

While much research, thus far, has focused on controlling the assembly and encapsulation properties of block copolymers and their corresponding assemblies,^{21–23} the functionalization of micelle and vesicle surfaces is emerging as an important area of research. The surfaces of the materials will come into direct contact with biological systems and will therefore play a critical role in determining their properties such as toxicity and biodistribution behavior.¹⁶ Furthermore, the conjugation of ligands to the surface can potentially lead to targeting of specific tissues such as tumors *in vivo*.^{24,25} Our group has recently reported a method for the introduction of dendritic groups to the surfaces of polymer vesicles using the widely applicable Cu(I)-catalyzed click reaction between vesicle azide groups and dendrons bearing focal point alkynes.²⁶ Owing to the high multivalency of the dendrons, this approach provides a rapid means of controlling the surface functionalities on the assembly. Furthermore, using mannose as a model biological ligand, it was demonstrated that binding to the target receptors was significantly enhanced using a dendritic approach in comparison to the conjugation of small molecules directly to the vesicle surface.²⁷ This result was also generalizable to polymer functionalized nanoparticles and was attributed to the increased

Additional Supporting Information may be found in the online version of this article. Correspondence to: E. R. Gillies (E-mail: egillie@uwo.ca)
Journal of Polymer Science Part A: Polymer Chemistry, Vol. 49, 2546–2559 (2011) © 2011 Wiley Periodicals, Inc.

SCHEME 1 Synthesis of HO-PEO-N₃ (**2**).

availability of the ligands on the surface of the nanomaterial when presented on the dendritic framework, as well as the clustered nature of the ligand display.

Overall, the results of our previous studies suggested that this dendritic surface functionalization approach is highly promising for controlling the surface functionalities of nanomaterials in order to impart specific biological properties and functions such as targeting. However, this initial work was performed on vesicles composed of poly(ethylene oxide)-*b*-polybutadiene (PEO-PBD), a nonbiodegradable polymer with unknown biocompatibility. Furthermore, the micron-scale sizes of these vesicles were unsuitable for *in vivo* circulation.²⁸ To address these limitations, and thus provide a significant advancement toward biomedical applications, we describe here the application of the dendritic surface functionalization approach to nanosized poly(ethylene oxide)-polycaprolactone (PEO-PCL) vesicles and micelles. PCL is a well-known biodegradable polymer that is currently FDA approved for uses in tissue engineering^{29,30} and drug delivery.^{31,32} Although PEO is not biodegradable, it is generally considered nontoxic and is currently used in several FDA-approved products, including PEG-INTRON, ONCASPAR, and NEULASTA. Both micelles^{33–39} and vesicles^{15,39–47} based on PEO-PCL have been previously reported and have been investigated as delivery vehicles for drugs such as doxorubicin,⁴¹ paclitaxel,¹⁵ docetaxel,³⁷ hemoglobin,⁴² dihydrotestosterone,³⁴ cyclosporine A,³⁵ and rapamycin.³⁶ In this work, we describe the synthesis of azide-terminated PEO-PCL block copolymers, their assembly into micelles and vesicles, and the conjugation of dendrons bearing different surface functionalities, including hydroxyls, amines, and guanidines, as well as a small molecule rhodamine derivative to both vesicles and micelles. The effects of these conjugations on the properties of the assemblies are explored.

RESULTS AND DISCUSSION

Synthesis of Block Copolymers

To functionalize polymer assemblies using the previously described azide + alkyne click chemistry approach, new PEO-PCL block copolymers bearing terminal azides on the hydrophilic PEO blocks were required. As the polymerization of ϵ -caprolactone is generally initiated from small molecule^{48,49} or macromolecular alcohols,^{50–52} these target copolymers could be most readily derived from asymmetrically functionalized PEOs bearing azide and hydroxyl termini (N₃-PEO-OH). While there are numerous reports describing the asymmetric functionalization of oligo(ethylene glycol)s,^{53–55} their higher MW analogues, particularly those lacking charged moieties are more difficult to prepare due to the purification challenges associated with statistical functionalization reactions. For example, in recent work,

Hillmyer and coworkers⁵⁶ did not succeed in purifying their target asymmetrically functionalized PEO and, therefore, used the statistical mixture of end-functionalized molecules in the preparation of a block copolymer. They later separated the resulting copolymers based on their differing solubilities and sizes. On the other hand, Taton and coworkers⁵⁷ have recently reported asymmetric PEOs that were obtained directly from the ring-opening polymerization of ethylene oxide using *N*-heterocyclic carbenes as catalysts.

In this work, to obtain the target N₃-PEO-OH, hydroxyl-terminated PEO (HO-PEO-OH, **1**) with a MW of 2000 g mol⁻¹ was first reacted with 1.1 equiv. of *p*-toluenesulfonyl chloride in the presence of 4-(dimethylamino)pyridine (DMAP) as a catalyst and NEt₃ (Scheme 1). The crude product was then reacted with sodium azide to obtain the target N₃-PEO-OH (**2**), along with the diazide N₃-PEO-N₃, and diol HO-PEO-OH resulting from the statistical functionalization. Although the properties of the three products were quite similar to each other, using very careful column chromatography, it was possible to isolate an 18% yield (out of a possible 50% theoretical yield) of the target compound **2** in pure form as evidenced by matrix-assisted laser desorption ionization (MALDI) mass spectrometry (Supporting Information). Despite the relatively low yield, the low cost of all of the reagents and starting materials for this chemistry resulted in this being a viable route for the preparation of the required macroinitiator.

As shown in Scheme 2, N₃-PEO-OH (**2**) was then used as a macroinitiator in the ring-opening polymerization of ϵ -caprolactone (CL). The commercially available PEO monomethyl ether (MeO-PEO-OH) was also used as a macroinitiator to provide block copolymers without terminal azides. These

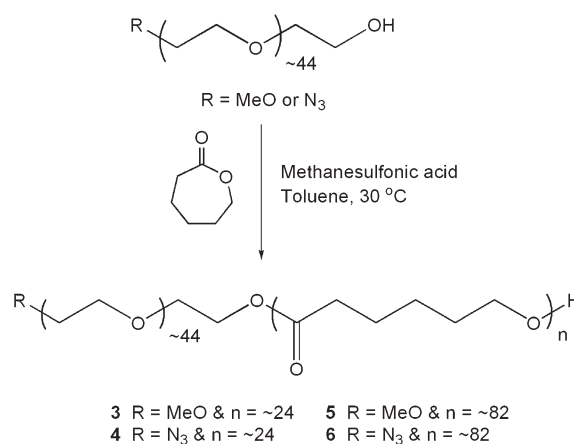
**SCHEME 2** Synthesis of PEO-PCL block copolymers.

TABLE 1 Molecular Weight Characteristics of PEO-PCL Block Copolymers

Copolymers	MW _{expected} (g mol ⁻¹) ^a	MW _{NMR} (g mol ⁻¹) ^b	M _w (g mol ⁻¹) ^c	PDI ^d	Yield (%)
MeO-PEO ₄₄ -PCL ₂₄ (3)	4,700	4,800	5,500	1.14	97
N ₃ -PEO ₄₄ -PCL ₂₄ (4)	4,700	5,000	4,600	1.18	97
MeO-PEO ₄₄ -PCL ₈₂ (5)	11,300	11,300	12,400	1.40	95
N ₃ -PEO ₄₄ -PCL ₈₂ (6)	11,300	11,600	12,000	1.19	93

^a Molecular weight expected from the polymerization based on the initiator and monomer ratio.

^b Molecular weight determined by ¹H NMR spectroscopy in CDCl₃.

^c Weight average molecular weight obtained from SEC-MALS.

^d Polydispersity index determined from SEC-MALS.

non-functionalized copolymers were required in the preparation of the assemblies to control the number of surface azide groups and, thus, the degree of functionalization with the dendritic groups. Most reports involving the preparation of PEO-PCL have involved the use of metal catalysts such as stannous(II) octanoate,^{38,43,45,58} zinc bis[bis(trimethylsilyl)amide],⁴⁰ or triethylaluminum.^{59–61} For *in vivo* applications, the use of nonmetallic catalysts is highly desired to minimize the potential toxicity effects. Acids such as HCl,^{37,62} trifluoromethanesulfonic acid,⁶³ and methanesulfonic acid⁶³ (MSA) have been reported to polymerize CL with small molecule alcohols as initiator. Among these catalysts, MSA was shown to produce PCLs with lower polydispersity indices (PDIs) and in shorter reaction times. For these reasons, MSA was selected as the catalyst for this work, and the polymerization was conducted at 30 °C for 2.5–3.5 h. Based on previous reports that PEO-PCL block copolymers with monomer ratios of approximately 44:9–44:40 assemble into spherical micelles, whereas those with ratios of 44:82–44:105 assemble into vesicles, the four block copolymers **3–6** shown in Table 1 were synthesized with the aim of preparing both micelles and vesicles from these materials.

The MWs of the resulting polymers were determined by ¹H NMR spectroscopy and size exclusion chromatography with detection by multi-angle light scattering (SEC-MALS). The MW characteristics of the synthesized block copolymers are summarized in Table 1, and SECs of the polymers are shown in Figure 1. It is worth noting that high reaction yields and relatively low polydispersity indices were generally obtained, with the measured MWs in agreement with target monomer ratios.

Synthesis of Alkyne Functionalized Dendrons

To explore the functionalization of the PEO-PCL vesicles and micelles, two different dendrons with focal point alkynes were initially explored. The third generation dendron **7** bearing peripheral amine functional groups and statistically one rhodamine dye per molecule was selected, as this dendron was used in previous work with the PEO-PBD vesicles²⁶ and would allow comparison between the different vesicle systems. Additionally, to demonstrate that the dendritic surface functionalization approach can impart new functions, the guanidine-functionalized dendron **9** was prepared by first reacting **7**²⁶ with the Boc-protected guanidine derivative **8**⁶⁴ in the presence of *O*-(benzotriazol-1-yl)-*N,N,N',N'*-

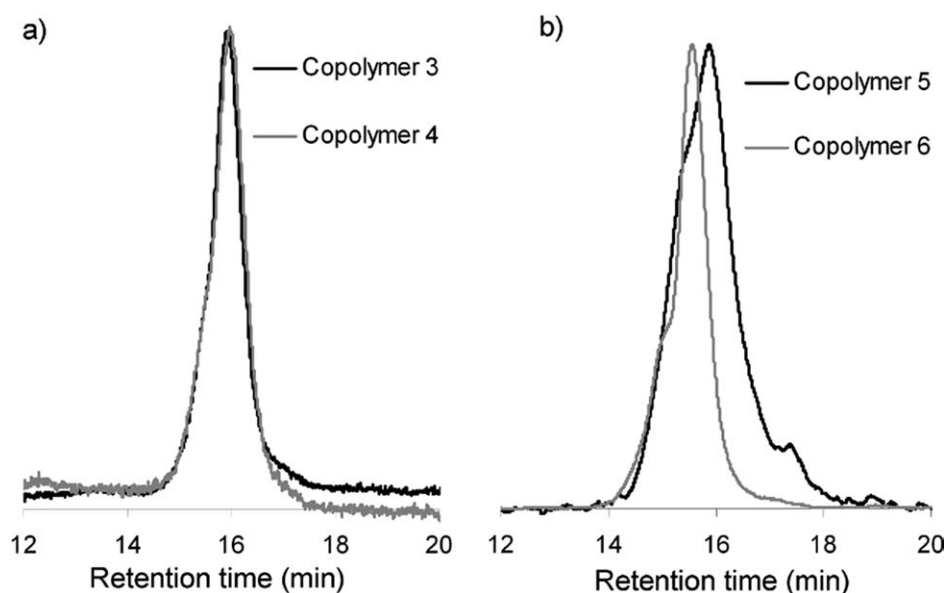
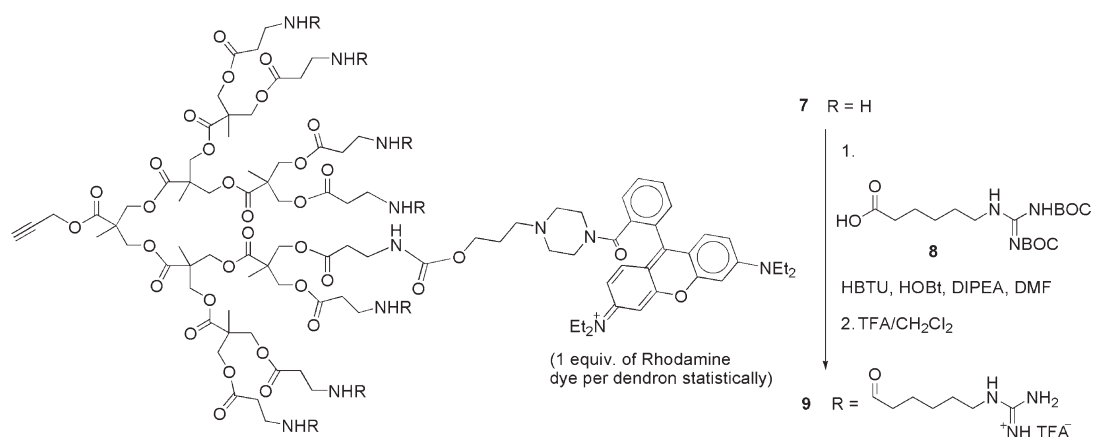


FIGURE 1 Size exclusion chromatography traces for copolymers: (a) **3** and **4** and (b) **5** and **6**. Detection was based on light scattering (90° trace shown).



SCHEME 3 Synthesis of rhodamine-labeled guanidine dendron **9**.

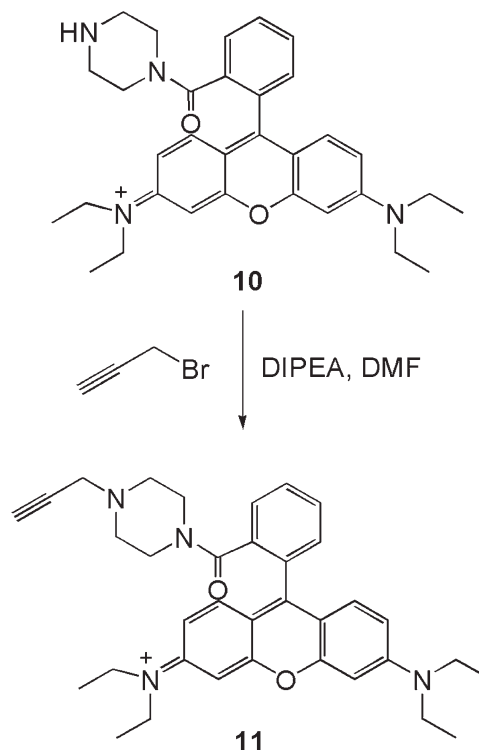
tetramethyluronium hexafluorophosphate (HBTU), 1-hydroxybenzotriazole (HOBT), and *N,N*-diisopropylethylamine (DIPEA), then removing the Boc groups by treatment with 1/1 trifluoroacetic acid (TFA)/CH₂Cl₂ (Scheme 3). Similar guanidine-functionalized dendrons⁶⁴ have been demonstrated by our group to have cell penetrating properties comparable to those of the well-known HIV Tat peptide^{65,66} and were capable of enhancing the transport of iron oxide nanoparticles into cells.⁶⁴ Therefore, they might enhance the capacity of these micelles and vesicles to carry cargo into cells. The extinction coefficients (ϵ) for dendrons **7** and **9** were determined by UV-visible spectroscopy to enable the quantification of their conjugation yields to the surfaces of the nanoassemblies. Finally, as the conjugation yields for the dendrons can be limited by steric hindrance at the surface of the assembly, it was also of interest to compare these reactions with those of a small molecule alkyne. Thus, the rhodamine derivative **10**⁶⁷ was reacted with propargyl bromide to provide **11** (Scheme 4). As the local environment of the dye may alter its extinction coefficient, rhodamine-functionalized derivatives of copolymers **4** and **6** were also prepared as shown in Scheme 5, and the extinction coefficients of the resulting polymers **12** and **13** were measured to enable the accurate quantification of the conjugation yields for **11**.

Formation of Nanoassemblies and Surface Functionalization Reactions

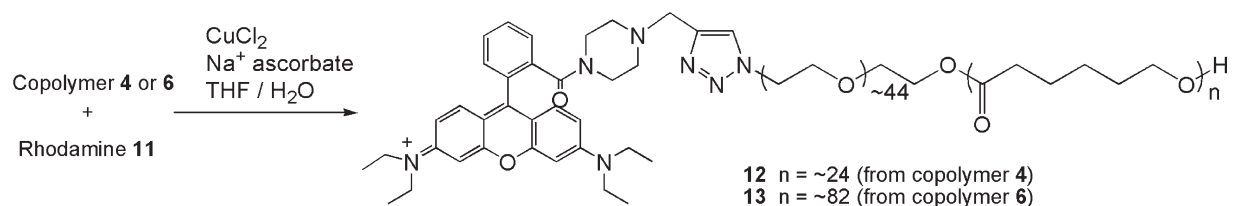
PEO-PCL vesicles and micelles can be formed through a number of different methods including rehydration of copolymer thin films on roughened teflon plates^{37,44,45} and nanoprecipitation.^{39,43,46,47} In our hands, thin-film rehydration of copolymers **3** and **4** provided micelles with diameters on the order of 25 nm. With copolymers **5** and **6**, rehydration of copolymer thin films on roughened teflon plates resulted in the formation of micron-sized vesicles, accompanied by many aggregates. The large sizes and aggregation were undesirable, so this method was not explored further. On the other hand, using a nanoprecipitation method involving the dissolution of the copolymer in tetrahydrofuran (THF), followed by a gradual addition of water and then dialysis against water to remove the THF, led reproducibly to

micelles with diameters of approximately 20 nm (copolymers **3** and **4**) and vesicles with diameters of approximately 140 nm (copolymers **5** and **6**) as measured by both dynamic light scattering (DLS) (Fig. 2) and transmission electron microscopy (TEM) (Fig. 3). As materials smaller than 100 nm are desired for *in vivo* applications, it was demonstrated that the vesicles could be extruded through a 100-nm polycarbonate membrane at 65 °C. This resulted in a decrease in the vesicle diameter to about 65 nm.

Micelles and vesicles with varying densities of surface azides were prepared from mixtures of copolymers **3** and **4** or **5** and **6**, respectively, using the nanoprecipitation method described above. Click reactions were subsequently



SCHEME 4 Synthesis of alkyne-functionalized rhodamine **11**.



SCHEME 5 Synthesis of rhodamine-labeled PEO-PCL block copolymers **12** and **13**.

performed using CuCl_2 , sodium ascorbate, and four equivalents of the alkyne **7**, **9**, or **11** relative to the azide (Scheme 6). After 18 h, the excess alkyne and other reagents were removed by dialysis. Following the removal of water, the materials resulting from each reaction were dissolved in $\text{CHCl}_3/\text{MeOH}$ (3/2), and their UV-visible absorbances were measured. Using the extinction coefficients measured for **7**, **9**, **12**, and **13**, the yields of the alkynes conjugated to the micelle and vesicle surfaces were then calculated.

The conjugation yields for the vesicles are shown in Figure 4(a). It was found that the yields for the conjugation of dendron **7**, bearing peripheral amines were very similar to those previously obtained with PEO-PBD vesicles.²⁶ It should be noted that approximately 50% of the azides should be located in the interior of the vesicles, and thus inaccessible to the dendron, which is unlikely to diffuse through the vesicle membrane. Nevertheless, as previously reported,²⁶ conjugation yields higher than 50% were obtained at low azide loadings. This may be attributed to the dynamic nature of the vesicles, allowing azides from the vesicle interior to migrate to the vesicle surface during the 18-h reaction time and then subsequently react. The slow migration of dendron **7** from the reaction solution into the vesicle core also cannot be excluded. To ensure that the high reaction yields were not the result of noncovalently immobilized dendron remaining after dialysis, a control experiment was also run on vesicles composed entirely of copolymer **5** but with the same excess of dendron and other reaction and purification conditions used for vesicles containing 10% copolymer **6**. In this case, the apparent “yield” was only ~1% indicating that no significant amount of noncovalently immobilized dendron remained after

dialysis. Therefore, noncovalently bound dendron would not explain the high reaction yields. As the azide loading increased beyond 20%, the reaction yields decreased. This was likely due to the steric hindrance at the vesicle surface, which restricted the conjugation of dendrons. The yields for the conjugation of the guanidine-functionalized dendron **9** were consistently lower than those for dendron **7**. This result was not surprising considering the larger size of this dendron.

Yields for the conjugation of the small molecule rhodamine derivative **11**, calculated using the extinction coefficient of **13**, were consistently greater than 90% for azide loadings of 1–40%. To ensure that the measured reaction yields accurately reflected covalently conjugated dye, and not simply dye entrapped within the vesicle core or membrane, these yields were determined following not only the usual aqueous dialysis but also a dialysis against *N,N*-dimethylformamide (DMF), which would disrupt the vesicles and enable the release of any noncovalently bound dye. Indeed, these yields are lower than those observed after just the aqueous dialysis, which were consistently greater than 100% (at all azide loadings). Furthermore, a control experiment performed on vesicles composed of copolymer **5** using the same reaction and purification conditions used for those containing 10% copolymer **6** showed that the apparent yield was only ~2%. This demonstrates the effectiveness of the multiple dialyses in removing all but trace amounts of noncovalently immobilized dye. Overall, these results suggested that the dye can diffuse across the vesicle membrane during the reaction time and react with azides on the interior membrane surface. Consistent with this hypothesis, we have observed the release of noncovalently encapsulated rhodamine out of

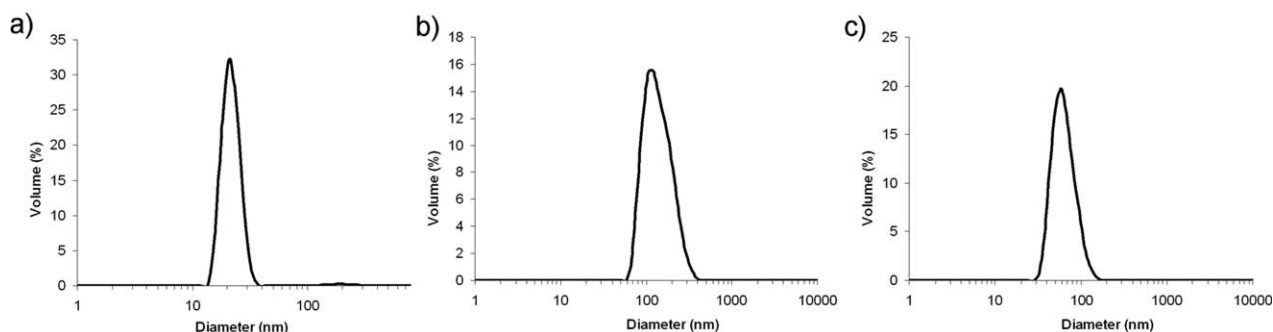


FIGURE 2 Size distribution profiles measured by dynamic light scattering for: (a) micelles prepared from copolymer **3**; (b) vesicles prepared from copolymer **5**; (c) extruded vesicles prepared from copolymer **5**.

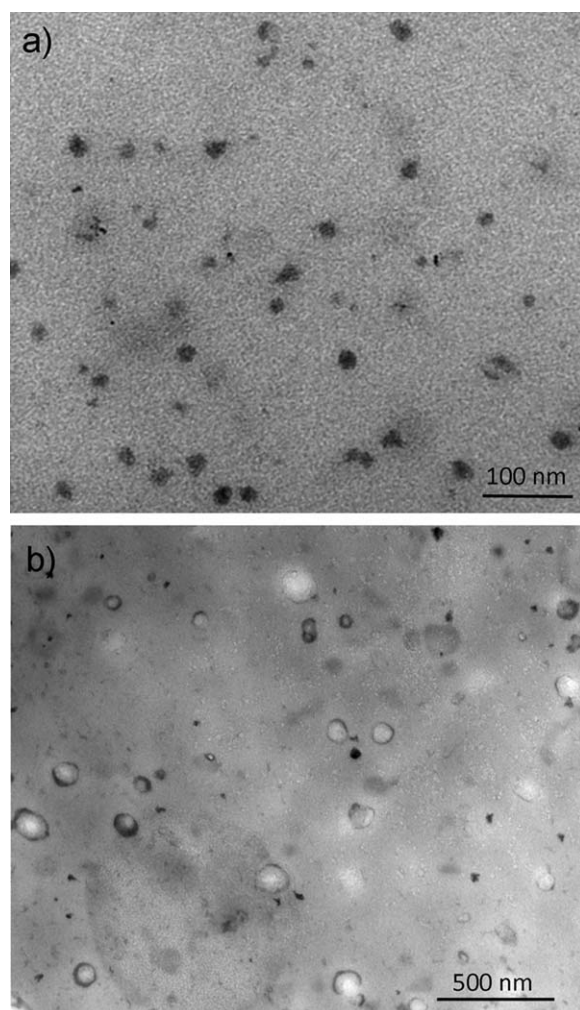
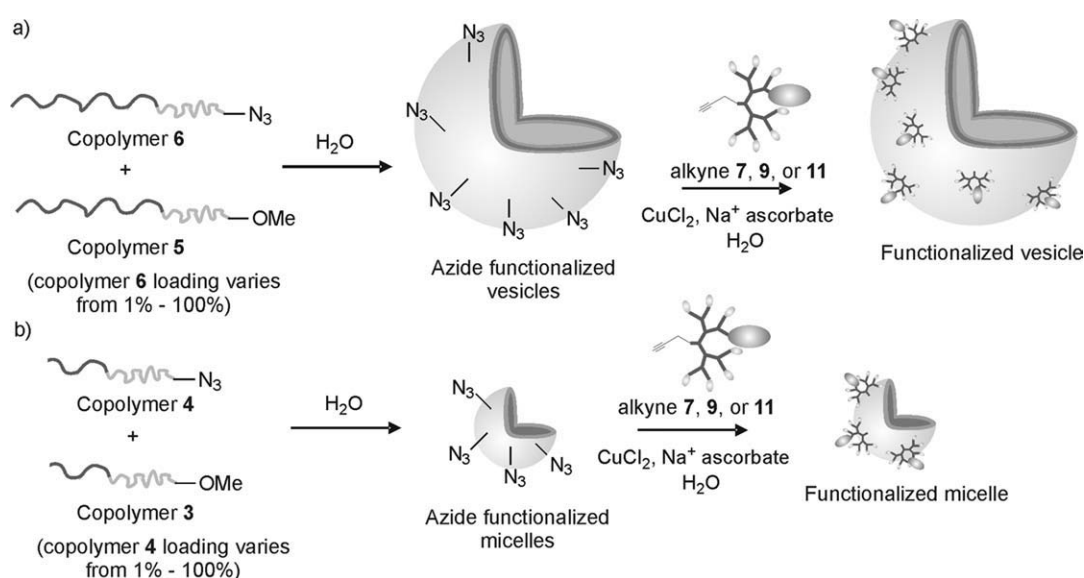


FIGURE 3 TEM images of (a) micelles prepared from copolymer **3** and (b) vesicles prepared from copolymer **5**.

vesicle cores over a 24-h period suggesting that the reverse process could also occur given the appropriate concentration gradient. Somewhat surprisingly, the reaction yields even for this small molecule dropped off at higher azide loadings above 20%. This might be attributed to the presence of dye molecules on the membrane disrupting the availability of nearby azides or perhaps due to diffusion of the rhodamine across the vesicle membrane providing insufficient concentrations of rhodamine to react with all of the azides at the vesicle core.

In the conjugation reactions of dendron **7** with the micelles, it was expected that the yields would approach 100% at low azide loadings, as all of the azides should be available for reaction at the micelles surface. However, as shown in Figure 4(b), this was not the case, and surprisingly, the conjugation yields were consistently lower than those obtained for the vesicles. The reasons for these lower yields are still unclear at this time but could perhaps be related to the large size of the dendrons relative to the micelles. The yields for the conjugation of the guanidine-functionalized dendron **9** were similar to those obtained with dendron **7** and were similar to the yields obtained on the vesicles. Like for the vesicles, the conjugation yields for the small molecule rhodamine **11** were high but unlike for the vesicles, these yields did not drop off as significantly at higher azide loadings. This suggests that the decrease in yields observed for the vesicles at high azide loading was more likely due to insufficient quantities of rhodamine **11** for reaction with the interior azides due to its limited diffusion across the vesicle membrane, rather than due to the presence of dye molecules hindering the reaction of nearby azides. Furthermore, in the context of the micelles, it suggests that the lower conjugation yields obtained for the dendrons were likely related to their size. It should also be noted that to investigate the reproducibility of the conjugation reactions, each reaction combination was



SCHEME 6 Preparation of functionalized (a) vesicles and (b) micelles.

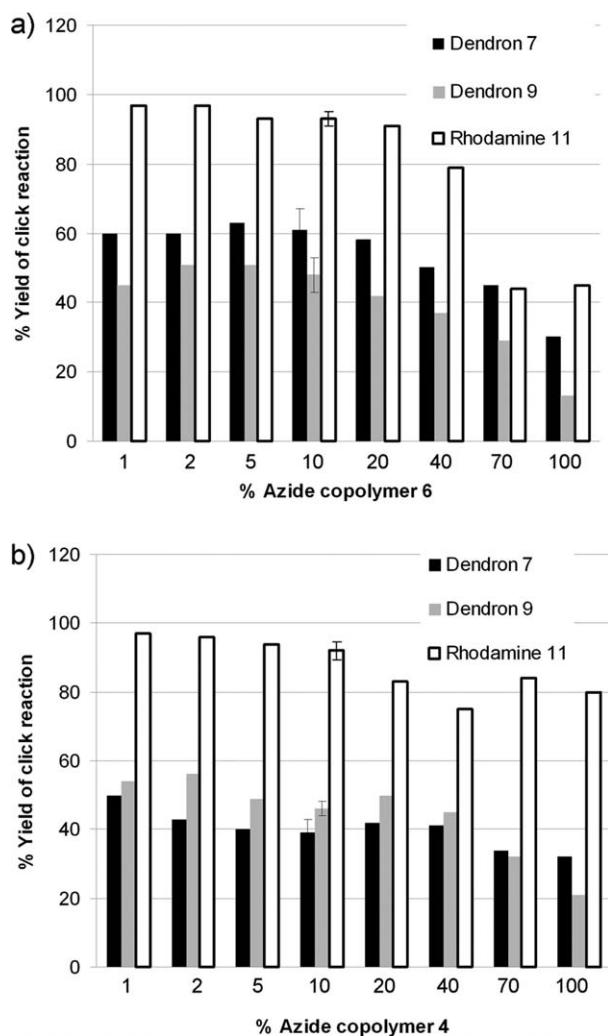


FIGURE 4 Click reaction yields as a function of azide loading on (a) vesicles (remaining copolymer is 5) and (b) micelles (remaining copolymer is 3).

repeated three times at the azide loading of 10%. The standard deviations, represented as error bars in Figure 4 ranged from ± 2 to $\pm 9\%$, indicating that the results were quite reproducible.

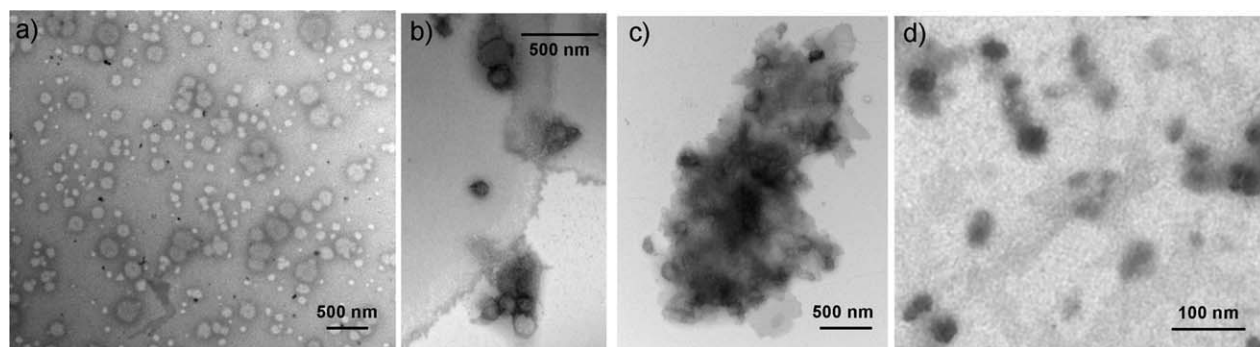


FIGURE 5 TEM images of (a) vesicles with 2% azide loading, following conjugation of dendron 9 (before dialysis); (b and c) vesicles with 2% azide loading, following conjugation of dendron 9 and dialysis, showing aggregation; (d) micelles with 20% azide loading, following conjugation of dendron 9 and dialysis.

Effects of Surface Functionalization on the Nanoassemblies

During the conjugation reactions, all of the micelles and vesicles remained well dispersed, and the solutions were clear. As shown in Figure 5(a,d), TEM confirmed that the micelles and vesicles remained intact following the click reaction. However, on removal of the excess alkyne and other reagents by aqueous dialysis, aggregation was observed in some cases. In the case of dendron 7 with the vesicles, DLS measurements revealed aggregation, even at low azide loadings [Fig. 6(a)], and beyond 10% azide loading, macroscopic aggregates were observed that could not even be measured by DLS. In our previous work with PEO-PBD, vesicle aggregates were observed at azide loadings beyond approximately 20%, but at low loadings, the vesicles remained well dispersed based on fluorescence confocal microscopy images.²⁶ Thus, the PEO-PCL vesicles appear to be more sensitive to aggregation. In the case of the guanidine dendron 9, the aggregation was even more extensive. The aggregates formed at 2% azide loading were detected by DLS [Fig. 6(a)] and were imaged by TEM [Fig. 5(b,c)]. Based on the TEM images, these aggregates seem to be composed primarily of vesicles. Beyond 2% azide, macroscopic precipitates were formed, and unfortunately, it was not possible to image these by TEM.

The high sensitivity of the vesicles to aggregation on dendron conjugation may be in part due to the resulting linear-dendritic copolymers being architecturally unfavorable for membrane formation. In addition, incorporation of the dendron may disrupt the hydrophilic-hydrophobic balance of the copolymer that is required for vesicle formation. These factors may destabilize the vesicle membrane. Nevertheless, the formation of the aggregates only on dialysis suggests that these are not the only factors. It is noteworthy that dendrons 7 and 9 both possess cationic charges and it is possible that the presence of the excess dendrons somehow help to stabilize the dispersed vesicles through hydrogen bonding or ionic interactions. To further investigate this aggregation phenomenon additional experiments were performed. First, a fourth generation polyester dendron 15 with a focal point alkyne was prepared as shown in Scheme 7.⁶⁸ This dendron was selected, as it was estimated to have a size similar to

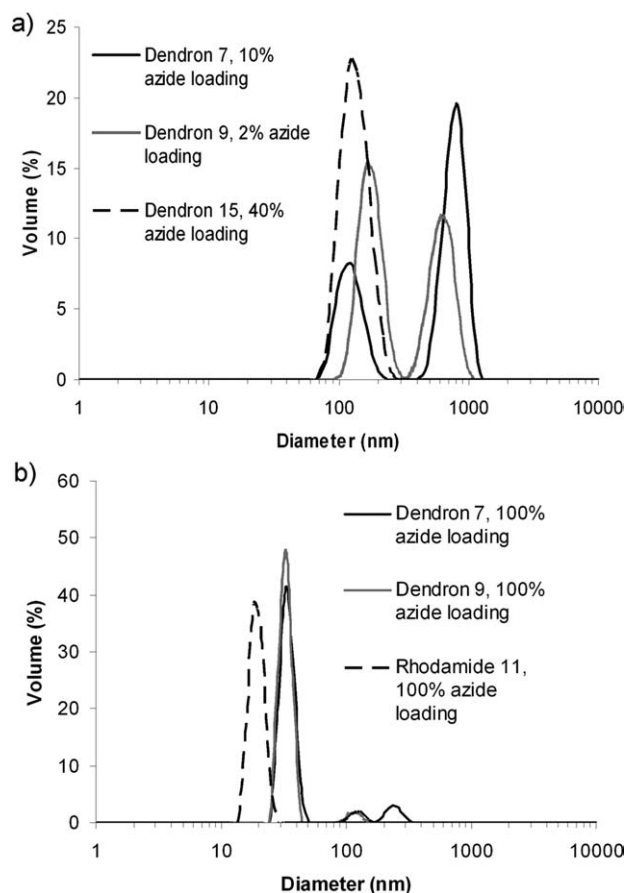
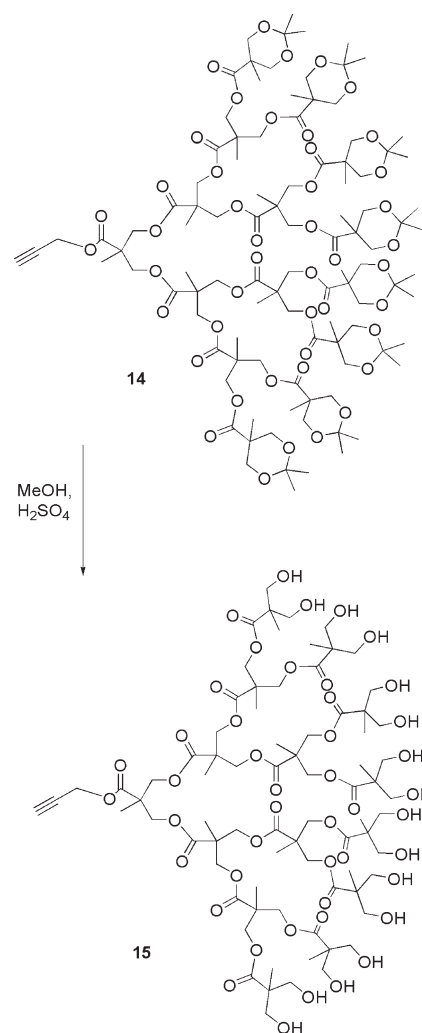


FIGURE 6 Size distribution profiles following click reactions and dialysis, measured by dynamic light scattering for (a) vesicles and (b) micelles.

dendron **7** but without the cationic charges. Dendron conjugation at azide loadings from 5% to 40% was investigated, and no aggregation was detected in any of these cases, even after dialysis [Fig. 6(a)]. This suggests that the dendritic architecture alone is not sufficient to trigger aggregation in this system, and that the charge of the dendrons was involved. The use of NaCl solutions (0.2 or 0.5 M) rather than pure water for the dialyses was also investigated as a means of controlling the counterion and ionic strength of the medium, but aggregation was still observed. Furthermore, dialyses using 0.1 M pH 6 phosphate buffer or 0.1 M pH 5 acetate buffer did not result in any detectable reduction in aggregation. The role of the rhodamine dye molecule was also investigated. Vesicles functionalized with alkyne **11**, did exhibit some aggregation, likely due to the dye's cationic charge, and the tendency of polycyclic aromatic systems to undergo π - π stacking (Supporting Information).⁶⁹ However, the rhodamine was certainly not the only contributor, as the conjugation of previously reported dendrons analogous to dendrons **7** and **9** but lacking the rhodamine^{26,64} led to the same degree of vesicle aggregation as observed with the dye-labeled dendrons. Therefore, it appears that the PEO-PCL vesicles are sensitive to aggregation, particularly on conjugation of cationic molecules. On the other hand, uncharged

dendritic molecules, despite their architecture, seem to be well tolerated and will be the focus of future work.

In the case of dendron conjugation to the micelles, much less aggregation was observed. For example, on conjugation of amine-functionalized dendron **7**, no significant aggregation was observed, even at azide loadings up to 100% [Fig. 6(b)]. The guanidine dendron **9** and the rhodamine **11** could also be conjugated at azide loadings up to 100% without significant aggregation [Fig. 6(b)]. Thus, overall the micelles were much less sensitive to aggregation than the vesicles. Unlike the vesicles, the incorporation of linear-dendritic polymers into micelles is known to be well tolerated, and there are several examples of micelles comprising linear dendritic copolymers where the dendritic block is hydrophilic or even hydrophobic.⁷⁰⁻⁷² Furthermore, micelle formation is generally favored for block copolymers possessing hydrophilic volume fractions of $>50\%$.⁸ Thus, the formation of micelles may be less affected by the increase in hydrophilic volume fraction imparted by the dendritic groups. The micelles also seem to be able to tolerate the introduction of charged groups much better than the vesicles. This may be attributed



SCHEME 7 Synthesis of dendron **15**.

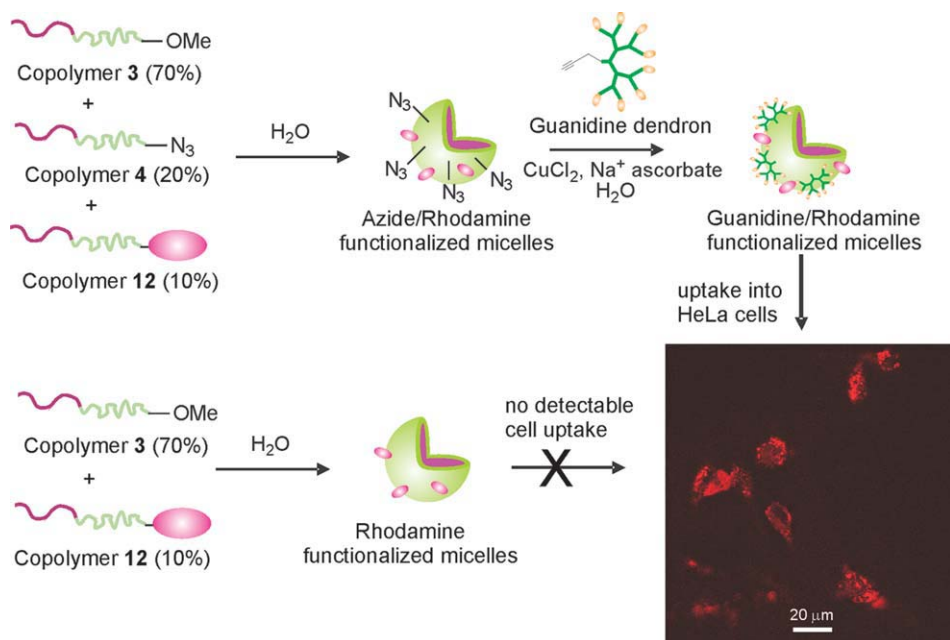


FIGURE 7 Preparation of PEO-PCL micelles functionalized with dendrons having peripheral guanidines, and their uptake into HeLa cells as visualized by fluorescence microscopy (detection of the rhodamine label). In contrast, micelles bearing the rhodamine label, but no dendron exhibited no detectable uptake.

to the inherent structural differences between the micelles and vesicles. If the introduction of cationic groups to the vesicle surfaces results in repulsive interactions that destabilize the membrane, the hydrophobic portions of the membranes can perhaps become exposed, triggering the aggregation. In contrast, the micelles possess much shorter hydrophobic blocks that are well buried at the cores of the micelles. This may make them inherently more resistant to the aggregation phenomena observed in this work.

Cellular Uptake of the Guanidine Dendron Functionalized Micelles

It has been shown by our group that dextran-coated superparamagnetic iron oxide nanoparticles bearing guanidine-functionalized polyester dendrons exhibit enhanced cell uptake relative to the unfunctionalized nanoparticles or those bearing hydroxyl or amine-functionalized dendrons.⁶⁴ To demonstrate that the dendritic surface functionalization approach can impart new functions to our nanoassemblies, the cellular uptake of micelles bearing guanidine functionalized dendrons was investigated in HeLa cancer cells. Micelles were prepared from a 70/20/10 ratio of polymers **3/4/12** as described above (Fig. 7). This provided an azide loading of 20% and the incorporation of polymer **12** provided the rhodamine for visualization of cell uptake. A dendron analogous to **9** but with an eighth guanidine in place of the rhodamine⁶⁴ was then conjugated to the micelle surface by the click chemistry protocol described above. This approach was used as the presence of the rhodamine dye in **9** might alter the transport properties of the dendron. Micelles comprising a 90/10 ratio of copolymers **3/12** were used as a control. Because of their high levels of aggregation, even at low azide loadings, guanidine-functionalized vesicles were not included in this experiment.

Micelles were incubated with the cells at a concentration of 0.1 mg mL⁻¹ (estimated 0.2 μM concentration of dendron) for 4 h, and then the cells were fixed and imaged by fluorescence confocal microscopy. As shown in Figure 7, cells incubated with the guanidine-functionalized micelles were strongly fluorescent, whereas no fluorescence was detected in cells incubated with the unfunctionalized micelles using the same microscope settings (Supporting Information). This suggests that the dendritic surface functionalization approach can be used to impart cell-penetrating properties to PEO-PCL micelles, which may allow them to more effectively deliver materials such as drugs, DNA, or labels into cells. Further experimentation will be required to quantify the cell uptake, study the intracellular tracking of these materials, and explore applications of these materials.

CONCLUSIONS

In conclusion, azide- and methoxy-terminated PEO-PCL block copolymers with the appropriate relative block lengths for formation of micelles and vesicles were prepared with the aim of developing surface-functionalized biodegradable assemblies. The azide- and methoxy-terminated copolymers were combined in varying ratios to provide assemblies with varying loadings of surface azide groups. Subsequently, dendrons having focal point alkyne moieties and peripheral amines, guanidines, or hydroxyl groups, as well as a small molecule alkyne derivative of rhodamine were conjugated to the surfaces of the micelles and vesicles using a Cu(I) catalyzed azide + alkyne cycloaddition reaction. It was found that the conjugation yields for the dendrons on the vesicles were similar to those reported previously for PEO-PBD vesicles, whereas those for the small molecule were higher, likely due to its ability to cross the vesicle membrane. Conjugation yields on the micelle surface were somewhat lower than expected for the dendrons but were high for the small

molecule. While the micelles remained well dispersed following all conjugation reactions, the vesicles exhibited a propensity to aggregate, particularly on the conjugation of cationic alkynes. To demonstrate the applicability of the dendritic surface functionalization approach, micelles with conjugated dendritic guanidines were shown to have enhanced cell uptake relative to unfunctionalized micelles.

EXPERIMENTAL

General Procedures and Materials

Chemicals were purchased from Sigma-Aldrich and were used without further purification unless otherwise noted. Anhydrous DMF, toluene, and CH_2Cl_2 were obtained from a solvent purification system. NEt_3 was distilled from CaH_2 . CL was stirred over CaH_2 for 24 h at room temperature and overnight at 60 °C, and then it was distilled from CaH_2 at reduced pressure under nitrogen immediately before polymerization. PEO derivatives were purified by precipitation from CH_2Cl_2 into cold diethyl ether (1:10). The precipitated PEO was then dried by azeotropic distillation ($\times 3$) with dry toluene using a Schlenk line system under nitrogen. Unless otherwise stated, all reactions were performed under a N_2 atmosphere using flame or oven dried glassware. Column chromatography was performed using silica gel (0.063–0.200-mm particle size, 70–230 mesh). Dialyses were performed using Spectra/Por regenerated cellulose membranes with either a 12,000–14,000 g mol^{-1} or 3500 g mol^{-1} molecular weight cutoff (MWCO). ^1H NMR spectra were obtained at 400 MHz, and ^{13}C NMR spectra were obtained at 100 MHz. NMR chemical shifts are reported in ppm and are calibrated against residual solvent signal of CDCl_3 (δ 7.26 and 77 ppm), CD_3OD (δ 3.34 ppm), or $(\text{CD}_3)_2\text{SO}$ (δ 2.50 and 40 ppm). Coupling constants (J) are expressed in Hertz (Hz). Infrared spectra were obtained as films from CH_2Cl_2 or THF/MeOH (5/1) on sodium chloride (NaCl) plates. UV-visible absorption spectroscopy was performed on a Varian Cary 300 Bio UV-visible spectrophotometer. Size exclusion chromatography (SEC) was performed in THF using a Waters 515 HPLC pump, Wyatt OptilabRex RI and miniDAWN-TREOS detectors, and two ResiPore (300 \times 7.5 mm) columns from Polymer Laboratories. Polymer MWs were calculated based on the MALS data using the Wyatt Astra software, with dn/dc values of the polymers determined from the RI detector using Astra. DLS data were obtained using a Zetasizer Nano ZS instrument from Malvern Instruments. MALDI-TOF mass spectrometry data were obtained using a 4700 Proteomics Analyzer, MALDI TOF TOF (Applied Biosystems, Foster City, CA). Reflectron and linear positive ion modes were used. High-resolution mass spectrometry (HRMS) was performed using a Finnigan MAT 8400 electron impact mass spectrometer. Extinction coefficients (ϵ) of compounds **7**, **9**, **11**, **12**, and **13** were obtained from calibration curves based on the measurement of UV-visible absorbance versus concentration in CHCl_3 /methanol (3/2).

Synthesis of N_3 -PEO-OH (**2**)

HO-PEO-OH (**1**) with a MW of 2000 g mol^{-1} (2.0 g, 1.0 mmol, 1.0 equiv.), *p*-toluenesulfonyl chloride (0.22 g, 1.1

mmol, 1.1 equiv.), and DMAP (0.061 g, 0.50 mmol, 0.50 equiv.) were dissolved in dry CH_2Cl_2 (30 mL). Dry NEt_3 (0.12 g, 1.2 mmol, 1.2 equiv.) was then added via syringe. The resulting mixture was stirred at room temperature for 24 h. Following this, the mixture was washed with cold 1-M HCl solution (1 \times 20 mL) and cold brine (1 \times 20 mL). The organic phase was dried over magnesium sulfate (MgSO_4). After removal of MgSO_4 via filtration, CH_2Cl_2 was removed under reduced pressure. The residue was taken up in minimal CH_2Cl_2 and the product was precipitated into cold diethyl ether. This material was then dissolved in dry DMF (15 mL). Sodium azide (0.16 g, 2.5 mmol, 2.5 equiv. relative to **1**) was then added, and the resulting mixture was stirred at 100 °C overnight. After cooling to room temperature, deionized water (15 mL), and CH_2Cl_2 (15 mL) were added. The organic phase was separated. The aqueous phase was extracted with CH_2Cl_2 (3 \times 10 mL), and the combined CH_2Cl_2 layers were dried over MgSO_4 . After removal of MgSO_4 via filtration, the CH_2Cl_2 was removed under reduced pressure. The residue was taken up in minimal CH_2Cl_2 and precipitated into cold diethyl ether. Subsequent purification by column chromatography using CH_2Cl_2 /MeOH as eluent (gradient: 19/1 to 14/1) gave compound **2** (0.36 g, 0.18 mmol) as a white solid.

Overall Yield: 18%. ^1H NMR (400 MHz, CDCl_3): δ 3.42–3.80 (m, 180H, $\text{CH}_2\text{—O—CH}_2$), 3.36 (t, 2H, $J = 4.0$ Hz, $\text{—CH}_2\text{—N}_3$). IR (film from CH_2Cl_2 , cm^{-1}): 3445 (O—H), 2884 (C—H), 2102 (N_3). MS calcd. for $[\text{M} + \text{Na}]^+$ based on functionalization of the starting polymer **1** with a peak MW of 1802 g mol^{-1} ($n = 40$): 1827. Found (MALDI-TOF+): 1827 (Supporting Information).

Synthesis of Copolymer 3 and General Procedure for the Preparation of Copolymers 3–6

Dry MeO-PEO-OH (0.25 g, 0.12 mmol, 1.0 equiv.) was added to a Schlenk flask as a solution in dry toluene (1.5 mL). CL (0.34 g, 3.0 mmol, 24 equiv.) was then added to the macroinitiator, and the resulting solution was equilibrated at 30 °C for 10 min. MSA (0.12 mmol, 7.8 μL , 1.0 equiv.) was then added, and the reaction mixture was stirred at 30 °C for 2.5 h. After cooling to room temperature, the mixture was treated with Amberlyst[®] A21 to remove the catalyst. The resin was removed by filtration, and the product was precipitated in excess cold hexane. The resulting white solid was filtered and dried *in vacuo* to give 0.57 g of the product.

Yield = 97%. ^1H NMR (400 MHz, CDCl_3): δ 4.21 (t, $J = 6.0$ Hz, 2H, $\text{—O—CH}_2\text{—CH}_2\text{—O—C(O)—}$), 4.05 (t, $J = 8.0$ Hz, 50H, $\text{—CH}_2\text{—O}$ in PCL block), 3.46–3.82 (m, 180H, $\text{—CH}_2\text{—O—CH}_2\text{—}$), 3.37 (s, 3H, —OCH_3), 2.29 (t, $J = 8.0$ Hz, 50H, $\text{—C(O)—CH}_2\text{—}$), 1.63 (m, 100H, $\text{—C(O)—CH}_2\text{—CH}_2\text{—CH}_2\text{—CH}_2\text{—CH}_2\text{—O—}$), 1.37 (m, 50H, $\text{—C(O)—CH}_2\text{—CH}_2\text{—CH}_2\text{—CH}_2\text{—CH}_2\text{—O—}$). IR (film from CH_2Cl_2 , cm^{-1}): 3436 (O—H), 2889 (C—H), 1724 (C=O). SEC: $M_w = 5500$ g mol^{-1} , PDI = 1.14, $dn/dc = 0.086$.

Synthesis of Copolymer 4

The copolymer was prepared by the same method described above for copolymer **3** except that compound **2** was used as

the macroinitiator. Yield = 97%. $^1\text{H NMR}$ (400 MHz, CDCl_3): δ 4.21 (t, $J = 6.0$ Hz, 2H, $-\text{O}-\text{CH}_2-\text{CH}_2-\text{O}-\text{C}(\text{O})-$), 4.05 (t, $J = 8.0$ Hz, 56H, $-\text{CH}_2-\text{O}$ in PCL block), 3.46–3.82 (m, 180H, $-\text{CH}_2-\text{O}-\text{CH}_2-$), 3.37 (t, $J = 6.0$ Hz, 2H, $-\text{CH}_2-\text{N}_3$), 2.29 (t, $J = 8.0$ Hz, 56H, $\text{C}(\text{O})-\text{CH}_2$), 1.63 (m, 112H, $-\text{C}(\text{O})-\text{CH}_2-\text{CH}_2-\text{CH}_2-\text{CH}_2-\text{CH}_2-\text{O}-$), 1.37 (m, 56H, $-\text{C}(\text{O})-\text{CH}_2-\text{CH}_2-\text{CH}_2-\text{CH}_2-\text{CH}_2-\text{O}-$). IR (film from CH_2Cl_2 , cm^{-1}): 3438 (O–H), 2869 (C–H), 2105 (N_3), 1724 (C=O). SEC: $M_w = 4600$ g mol^{-1} , PDI = 1.18, $dn/dc = 0.078$.

Synthesis of Copolymer 5

The copolymer was prepared by the same method described above for copolymer **3** except that 82 equiv. of CL were used and the reaction time was 3.5 h. Yield = 95%. $^1\text{H NMR}$ (400 MHz, CDCl_3): δ 4.19 (t, $J = 6.0$ Hz, 2H, $-\text{O}-\text{CH}_2-\text{CH}_2-\text{O}-\text{C}(\text{O})-$), 4.03 (t, $J = 8.0$ Hz, 164H, $-\text{CH}_2-\text{O}$ in PCL block), 3.43–3.79 (m, 180H, $-\text{CH}_2-\text{O}-\text{CH}_2-$), 3.35 (s, 3H, $-\text{OCH}_3$), 2.28 (t, $J = 8.0$ Hz, 164H, $-\text{C}(\text{O})-\text{CH}_2-$), 1.64 (m, 328H, $-\text{C}(\text{O})-\text{CH}_2-\text{CH}_2-\text{CH}_2-\text{CH}_2-\text{CH}_2-\text{O}-$), 1.37 (m, 164H, $-\text{C}(\text{O})-\text{CH}_2-\text{CH}_2-\text{CH}_2-\text{CH}_2-\text{CH}_2-\text{O}-$). IR (film from CH_2Cl_2 , cm^{-1}): 3437 (O–H), 2867 (C–H), 1724 (C=O). SEC: $M_w = 12,400$ g mol^{-1} , PDI = 1.40, $dn/dc = 0.060$.

Synthesis of Copolymer 6

The copolymer was prepared by the same method described above for copolymer **3** except that compound **2** was used as the macroinitiator, 82 equiv. of CL were used, and the reaction time was 3.5 h. Yield = 93%. $^1\text{H NMR}$ (400 MHz, CDCl_3): δ 4.21 (t, $J = 6.0$ Hz, 2H, $-\text{O}-\text{CH}_2-\text{CH}_2-\text{O}-\text{C}(\text{O})-$), 4.05 (t, $J = 8.0$ Hz, 168H, $-\text{CH}_2-\text{O}-$ in PCL block), 3.45–3.80 (m, 180H, $-\text{CH}_2-\text{O}-\text{CH}_2-$), 3.38 (t, $J = 4.0$ Hz, 2H, $-\text{CH}_2-\text{N}_3$), 2.30 (t, $J = 8.0$ Hz, 168H, $-\text{C}(\text{O})-\text{CH}_2$), 1.64 (m, 336H, $-\text{C}(\text{O})-\text{CH}_2-\text{CH}_2-\text{CH}_2-\text{CH}_2-\text{CH}_2-\text{O}-$), 1.37 (m, 168H, $-\text{C}(\text{O})-\text{CH}_2-\text{CH}_2-\text{CH}_2-\text{CH}_2-\text{CH}_2-\text{O}-$). IR (film from CH_2Cl_2 , cm^{-1}): 3433 (O–H), 2866 (C–H), 2100 (N_3), 1725 (C=O). SEC: $M_w = 12,000$ g mol^{-1} , PDI = 1.19, $dn/dc = 0.080$.

Synthesis of Dendron 9

Dendron **7**²⁶ (81 mg, 39 μmol , 1.0 equiv.) and the protected guanidine derivative **8**⁶⁴ (0.20 g, 0.55 mmol, 14 equiv.) were dissolved in anhydrous DMF (7 mL) under a nitrogen atmosphere. HBTU (0.20 g, 0.55 mmol, 14 equiv.) was added, followed by HOBt (73 mg, 0.55 mmol, 14 equiv.) and DIPEA (0.14 mL, 0.78 mmol, 20 equiv.). The reaction mixture was stirred under nitrogen in the dark for 48 h. The product was then purified by dialysis against DMF using a 3500 MWCO membrane for 24 h. After removal of DMF under reduced pressure, the residue was dissolved in 2 mL of 1/1 TFA/ CH_2Cl_2 , and the reaction mixture was stirred at room temperature and in dark for 2 h. The solvent was removed under reduced pressure to provide dendron **9** (0.11 g) with approximately one chromophore per dendron statistically.

Yield: 87%. $^1\text{H NMR}$ (400 MHz, CD_3OD): δ 7.92 (d, $J = 8.0$ Hz, 1H, dye aromatic), 7.84–7.75 (m, 3H, dye aromatic), 7.65–7.47 (m, 3H, dye aromatic), 7.28 (d, $J = 12$ Hz, 1H, dye aromatic), 7.10 (dd, $J = 4.0$ Hz and 12 Hz, 1H, dye aromatic), 7.00 (d, $J = 4.0$ Hz, 1H, dye aromatic), 4.84–4.81 (m, 2H,

dendron $-\text{C}(\text{O})-\text{O}-\text{CH}_2$ -alkyne), 4.39–4.10 (m, 30H, dendron $-\text{C}(\text{O})-\text{C}-\text{CH}_2-\text{O}$, dye $-\text{CH}_2-\text{C}(\text{O})\text{O}$), 3.78–3.65 (m, 8H, dye $-\text{C}(\text{O})-\text{N}-\text{CH}_2$), 3.55–3.37 (m, 20H, dendron $-\text{CH}_2\text{NHC}(\text{O})$, dye $-\text{C}(\text{O})-\text{N}-\text{CH}_2$), 3.20 (t, $J = 8.0$ Hz, 16H, dendron $-\text{CH}_2$ -guanidine), 3.04 (br s, 1H, terminal alkyne), 2.76–2.68 (m, 2H, dye $-\text{O}-\text{CH}_2\text{CH}_2\text{CH}_2-\text{N}$), 2.66–2.47 (m, 16H, dendron $-\text{C}(\text{O})-\text{CH}_2\text{CH}_2\text{NH}-$), 2.48–2.21 (m, 20H, dendron $-\text{NHC}(\text{O})\text{CH}_2-$, dye $-\text{C}(\text{O})-\text{N}-\text{CH}_2-\text{CH}_2$), 1.81–1.55 (m, 32H, dendron $-\text{NHC}(\text{O})\text{CH}_2\text{CH}_2\text{CH}_2\text{CH}_2\text{CH}_2$ -guan), 1.52–1.07 (m, 49H, dendron $-\text{NHC}(\text{O})\text{CH}_2\text{CH}_2\text{CH}_2\text{CH}_2\text{CH}_2$ -guan, dendron $-\text{C}(\text{O})-\text{C}-\text{CH}_3$, dye Ar-N- $-\text{CH}_2-\text{CH}_3$). IR (film from THF/MeOH, cm^{-1}): 3282 (N–H), 3180 (N–H), 2943 (C–H), 2125 (C \equiv C), 1730 (C=O ester), 1670 (C=O amide), 1590 (C=C aromatic), 1467 (C=C aromatic). Extinction coefficient (ϵ): 28,008 L mol^{-1} cm^{-1} at 563 nm ($\text{CHCl}_3/\text{MeOH}$, 3/2).

Synthesis of Rhodamine Derivative 11

To a solution of **10**⁶⁷ (0.40 g, 0.73 mmol, 1.0 equiv.) in anhydrous DMF (2 mL) were added propargyl bromide (0.11 g, 0.92 mmol, 1.2 equiv.) and DIPEA (0.16 g, 1.3 mmol, 1.8 equiv.). The reaction mixture was stirred at room temperature in the dark for 24 h. An additional 1.2 equiv. of propargyl bromide and DIPEA was then added, and the resulting solution was stirred for 2 additional h. The reaction mixture was then partitioned between ethyl acetate and saturated aqueous NaHCO_3 . The aqueous layer was extracted with isopropanol/ CH_2Cl_2 (1/3). The organic layer was collected, dried over MgSO_4 , filtered, and concentrated to provide 0.33 g of the desired product. Yield: 82%. $^1\text{H NMR}$ (400 MHz, CDCl_3): δ 7.69–7.67 (m, 2H, *ortho* to NEt_2 and O), 7.56–7.54 (m, 1H, phenyl), 7.37–7.35 (m, 1H, phenyl), 7.28 (s, 1H, phenyl), 7.25 (s, 1H, phenyl), 7.05–7.02 (dd, $J = 4.0$ Hz and 12 Hz, 2H, *ortho* to NEt_2), 6.81 (d, $J = 4.0$ Hz, 2H, *meta* to NEt_2), 3.71–3.61 (m, 8H, Ar-N- $-\text{CH}_2-$), 3.46–3.41 (m, 2H, $-\text{C}(\text{O})-\text{N}-\text{CH}_2-$), 3.38–3.32 (m, 2H, $-\text{C}(\text{O})-\text{N}-\text{CH}_2-$), 3.26 (d, $J = 4.0$ Hz, 2H, $-\text{N}-\text{CH}_2$ -alkyne), 2.41–2.33 (m, 4H, $-\text{C}(\text{O})-\text{N}-\text{CH}_2-\text{CH}_2-$), 2.24 (t, $J = 4.0$ Hz, 1H, terminal alkyne), 1.33 (t, $J = 8.0$ Hz, 12H, Ar-N- $-\text{CH}_2-\text{CH}_3$). $^{13}\text{C NMR}$ (400 MHz, CDCl_3): δ 167.2, 157.5, 155.4, 135.2, 131.8, 130.2, 130.0, 129.7, 127.4, 114.0, 113.4, 110.7, 96.1, 73.8, 51.4, 50.7, 47.2, 46.4, 46.0, 41.3, 12.5. HRMS (m/z) calcd for $\text{C}_{35}\text{H}_{42}\text{N}_4\text{O}_2$, 550.3308; found (ESI), 550.3221 [M]⁺. Extinction coefficient (ϵ): 86,201 L mol^{-1} cm^{-1} at 563 nm ($\text{CHCl}_3/\text{MeOH}$, 3/2).

Preparation of Rhodamine Labeled Copolymers 12 and 13

Copolymer **4** or **6** (1.0 equiv.) and rhodamine derivative **11** (5.0 equiv.) were dissolved in THF/ H_2O (2/1). To the solution were added $\text{CuCl}_2 \cdot 2\text{H}_2\text{O}$ (5.0 equiv.) and sodium ascorbate (50 equiv.), and the reaction mixture was stirred in the dark at room temperature for 20 h. The product was purified by first dialysis against distilled water for 24 h followed by dialysis against DMF for an additional 24 h using a 3500 MWCO dialysis membrane. DMF was removed *in vacuo* to give dye-labeled polymers **12** (yield: 81%) or **13** (yield: 89%), respectively. Because of the low intensity of aromatic peaks of the dye compared to the polymer peaks, the

integration of the ^1H NMR spectrum was not possible. However, completion of the reaction was confirmed by disappearance of the peaks corresponding to the methylene protons adjacent to the azide group in the polymer (Supporting Information). Extinction coefficient (ϵ) for **12**: $22,851 \text{ L mol}^{-1} \text{ cm}^{-1}$ at 563 nm ($\text{CHCl}_3/\text{MeOH}$, 3/2). Extinction coefficient (ϵ) for **13**: $19,847 \text{ L mol}^{-1} \text{ cm}^{-1}$ at 563 nm ($\text{CHCl}_3/\text{MeOH}$, 3/2).

Synthesis of Dendron 15

Dendron **14**⁶⁸ (0.42 g, 0.20 mmol) was dissolved in methanol (150 mL), and concentrated sulfuric acid (1.5 mL) was added. The resulting solution was stirred at room temperature for 2 h and then was then neutralized with 7 M NH_3 in MeOH to pH 7. The solution was filtered to remove the $(\text{NH}_4)_2\text{SO}_4$ precipitate, and then the solvent was removed under reduced pressure to provide **15** (0.35 g) as a white solid.

Yield: 99%. ^1H NMR (400 MHz, $\text{DMSO}-d_6$): δ 7.35–6.80 (br s, 16H, $-\text{OH}$), 4.72 (d, $J = 7.8 \text{ Hz}$, 2H, alkyne- CH_2-O), 4.70–4.50 (m, 12H, $-\text{C}(\text{O})-\text{C}-\text{CH}_2-\text{O}-$ from first and second generations), 4.21–4.07 (m, 16H, $-\text{C}(\text{O})-\text{C}-\text{CH}_2-\text{O}-$ from third generation), 3.49–3.30 (m, 32H, $-\text{C}(\text{O})-\text{C}-\text{CH}_2-\text{OH}$), 2.42 (t, $J = 7.0 \text{ Hz}$, 1H, terminal alkyne), 1.22 (s, 3H, $-\text{C}(\text{O})-\text{C}-\text{CH}_3$ from first generation), 1.18 (s, 6 H, $-\text{C}(\text{O})-\text{C}-\text{CH}_3$ from second generation), 1.15 (s, 12H, $-\text{C}(\text{O})-\text{C}-\text{CH}_3$ from third generation), 1.00 (s, 24H, $-\text{C}(\text{O})-\text{C}-\text{CH}_3$ from fourth generation). ^{13}C NMR (400 MHz, $\text{DMSO}-d_6$): δ 174.5, 172.2, 171.8, 171.7, 78.3, 78.2, 64.8, 64.1, 53.3, 50.6, 46.7, 46.6, 33.7, 25.7, 24.9, 17.8, 17.6, 17.3, 17.1. MS (m/z) calcd for $\text{C}_{78}\text{H}_{124}\text{NaO}_{46}$, 1820; found (MALDI-TOF), 1820 [$\text{M} + \text{Na}$]⁺.

General Procedure for the Preparation of PEO-PCL Micelles and Vesicles

The block copolymer (5 mg) was dissolved in THF (0.5 mL). DI water (2 mL) was added dropwise over 10 min. with vigorous stirring. After the addition was complete, the resulting nanoassembly suspension was stirred for 10 min. and then dialyzed against 2 L of distilled water, using a 12,000–14,000 MWCO dialysis membrane, with multiple changes for at least 36 h to remove THF. The vesicles were extruded 10 times through a 0.1- μm polycarbonate membrane at 65 °C using a pressure driven Lipex Thermobarrel Extruder (1.5 mL capacity, Northern Lipids).

General Procedure for Surface Functionalization of Micelles and Vesicles

Micelles or vesicles were prepared as described above using mixtures of copolymers **3** and **4** (micelles) or **5** and **6** (vesicles) in varying ratios (Scheme 6). To the assemblies were added $\text{CuCl}_2 \cdot 2\text{H}_2\text{O}$ (0.40 equiv. relative to total polymer), sodium ascorbate (4.0 equiv. relative to total polymer), and dye-labeled dendron **7**, **9** or dye **11** (4.0 equiv. relative azides) in sequence, and the reaction mixture was stirred at room temperature for 18 h and then dialyzed against distilled water for 24 h using a 12,000–14,000 MWCO or 3500 MWCO dialysis membrane.

Quantification of Surface Dendritic Groups

Following dialysis, the samples were lyophilized to remove water and were then taken up in about 2 mL of $\text{CHCl}_3/\text{methanol}$ 3/2. The solutions were centrifuged at 4500 rpm for 4 h to remove any insoluble material. Finally, the absorbance was measured at 563 nm. The degree of functionalization was calculated using the measured ϵ for the dye-labeled dendron **7**, dye-labeled guanidine dendron **9**, or rhodamine-functionalized polymers **12** or **13** in the same solvent.

Transmission Electron Microscopy

The suspension of micelles or vesicles (20 μL , 0.1 mg mL^{-1}) was placed on a carbon formvar grid and was left to stand for 5 min. The excess solution was then blotted off using a piece of filter paper. The resulting sample was dried in air overnight before imaging. Imaging was performed using a Phillips CM10 microscope operating at 80 kV with a 40 μm aperture.

Uptake of Micelles into HeLa Cells

HeLa cells were maintained at 37 °C and 5% CO_2 in Dulbecco's Modified Eagle Medium (Invitrogen) supplemented with 10% fetal bovine serum (Invitrogen). Sterilized microscope glass cover slips (22mm \times 22mm) were placed in the wells of a 6-well plate and 1.5×10^5 cells per well were seeded onto each cover slip. The cells were allowed to adhere for 24 h. The culture medium was then aspirated and replaced with fresh serum-free medium containing control or functionalized micelles at a concentration of 0.1 mg mL^{-1} of polymer. The experiments were completed in triplicate. The cells were incubated at 37 °C for 4 h. They were then washed three times with phosphate-buffered saline (PBS) then fixed with 10% paraformaldehyde solution for 10 min. The cells were washed again with PBS, and then the cover slips were placed face down onto microscope slides for confocal microscopy. Confocal images were obtained using a confocal laser scanning microscope (LSM 510, Carl Zeiss) using a 63 \times (N.A. = 1.4) oil immersion objective and an excitation wavelength of 543 nm (He-Ne laser).

The authors thank the Natural Sciences and Engineering Research Council of Canada and the Government of Ontario Ministry of Research and Innovation for funding this work.

REFERENCES AND NOTES

- Alexandridis, P.; Lindman, B. *Amphiphilic Block Copolymers: Self-Assembly and Applications*; Elsevier: Amsterdam: New York, 2000.
- Cornelissen, J.; Fischer, M.; Sommerdijk, N.; Nolte, R. J. M. *Science* 1998, 280, 1427–1430.
- Pochan, D. J.; Chen, Z. Y.; Cui, H. G.; Hales, K.; Qi, K.; Wooley, K. L. *Science* 2004, 306, 94–97.
- Zhang, L. F.; Eisenberg, A. *Science* 1995, 268, 1728–1731.
- Discher, D. E.; Eisenberg, A. *Science* 2002, 297, 967–973.
- Yan, D. Y.; Zhou, Y. F.; Hou, J. *Science* 2004, 303, 65–67.

- 7 Cui, H. G.; Chen, Z. Y.; Zhong, S.; Wooley, K. L.; Pochan, D. *J. Science* 2007, 317, 647–650.
- 8 Ahmed, F.; Photos, P. J.; Discher, D. E. *Drug Dev Res* 2006, 67, 4–14.
- 9 Photos, P. J.; Bacakova, L.; Discher, B.; Bates, F. S.; Discher, D. E. *J Controlled Release* 2003, 90, 323–334.
- 10 Zhang, S. Y.; Zhao, Y. *J Am Chem Soc* 2010, 132, 10642–10644.
- 11 Ranquin, A.; Versees, W.; Meier, W.; Steyaert, J.; Van Gelder, P. *Nano Lett* 2005, 5, 2220–2224.
- 12 Toti, U. S.; Guru, B. R.; Grill, A. E.; Panyam, J. *Mol Pharm* 2010, 7, 1108–1117.
- 13 Liu, G. J.; Ma, S. B.; Li, S. K.; Cheng, R.; Meng, F. H.; Liu, H. Y.; Zhong, Z. Y. *Biomaterials* 2010, 31, 7575–7585.
- 14 Harada, A.; Togawa, H.; Kataoka, K. *Eur J Pharm Sci* 2001, 13, 35–42.
- 15 Ahmed, F.; Pakunlu, R. I.; Srinivas, G.; Brannan, A.; Bates, F.; Klein, M. L.; Minko, T.; Discher, D. E. *Mol Pharm* 2006, 3, 340–350.
- 16 Yang, X. Q.; Grailer, J. J.; Rowland, I. J.; Javadi, A.; Hurley, S. A.; Matson, V. Z.; Steeber, D. A.; Gong, S. Q. *ACS Nano* 2010, 4, 6805–6817.
- 17 Yang, X. Q.; Grailer, J. J.; Rowland, I. J.; Javadi, A.; Hurley, S. A.; Steeber, D. A.; Gong, S. Q. *Biomaterials* 2010, 31, 9065–9073.
- 18 Ghoroghchian, P. P.; Frail, P. R.; Susumu, K.; Blessington, D.; Brannan, A. K.; Bates, F. S.; Chance, B.; Hammer, D. A.; Therien, M. J. *Proc Natl Acad Sci USA* 2005, 102, 2922–2927.
- 19 Guthi, J. S.; Yang, S. G.; Huang, G.; Li, S. Z.; Khemtong, C.; Kessinger, C. W.; Peyton, M.; Minna, J. D.; Brown, K. C.; Gao, J. M. *Mol Pharm* 2010, 7, 32–40.
- 20 Chen, D. Y.; Li, N. J.; Gu, H. W.; Xia, X. W.; Xu, Q. F.; Ge, J. F.; Lu, J. M.; Li, Y. G. *Chem Commun* 2010, 46, 6708–6710.
- 21 Blanz, A.; Armes, S. P.; Ryan, A. J. *Macromol Rapid Commun* 2009, 30, 267–277.
- 22 LoPresti, C.; Lomas, H.; Massignani, M.; Smart, T.; Battaglia, G. *J Mater Chem* 2009, 19, 3576–3590.
- 23 Letchford, K.; Burt, H. *Eur J Pharm Biopharm* 2007, 65, 259–269.
- 24 Pittet, M. J.; Swirski, F. K.; Reynolds, F.; Josephson, L.; Weissleder, R. *Nat Protoc* 2006, 1, 73–79.
- 25 Pang, Z. Q.; Feng, L. A.; Hua, R. R.; Chen, J.; Gao, H. L.; Pan, S. Q.; Jiang, X. G.; Zhang, P. *Mol Pharm* 2010, 7, 1995–2005.
- 26 Li, B.; Martin, A. L.; Gillies, E. R. *Chem Commun* 2007, 5217–5219.
- 27 Martin, A. L.; Li, B.; Gillies, E. R. *J Am Chem Soc* 2009, 131, 734–741.
- 28 Shi, M.; Lu, J.; Shoichet, M. S. *J Mater Chem* 2009, 19, 5485–5498.
- 29 Lam, C. X. F.; Teoh, S. H.; Hutmacher, D. W. *Polym Int* 2007, 56, 718–728.
- 30 Jenkins, M. J.; Harrison, K. L.; Silva, M.; Whitaker, M. J.; Shakesheff, K. M.; Howdle, S. M. *Eur Polym J* 2006, 42, 3145–3151.
- 31 Sinha, V. R.; Bansal, K.; Kaushik, R.; Kumria, R.; Trehan, A. *Int J Pharm* 2004, 278, 1–23.
- 32 Chandra, R.; Rustgi, R. *Prog Polym Sci* 1998, 23, 1273–1335.
- 33 Allen, C.; Yu, Y. S.; Maysinger, D.; Eisenberg, A. *Bioconjugate Chem* 1998, 9, 564–572.
- 34 Allen, C.; Han, J. N.; Yu, Y. S.; Maysinger, D.; Eisenberg, A. *J Controlled Release* 2000, 63, 275–286.
- 35 Aliabadi, H. M.; Mahmud, A.; Sharifabadi, A. D.; Lavasanifar, A. *J Controlled Release* 2005, 104, 301–311.
- 36 Forrest, M. L.; Won, C. Y.; Malick, A. W.; Kwon, G. S. *J Controlled Release* 2006, 110, 370–377.
- 37 Mikhail, A. S.; Allen, C. *Biomacromolecules* 2010, 11, 1273–1280.
- 38 Azzam, T.; Eisenberg, A. *Langmuir* 2007, 23, 2126–2132.
- 39 Adams, D. J.; Kitchen, C.; Adams, S.; Fuzeland, S.; Atkins, D.; Schuetz, P.; Fernyhough, C. M.; Tzokova, N.; Ryan, A. J.; Butler, M. F. *Soft Matter* 2009, 5, 3086–3096.
- 40 Meng, F. H.; Hiemstra, C.; Engbers, G. H. M.; Feijen, J. *Macromolecules* 2003, 36, 3004–3006.
- 41 Ahmed, F.; Discher, D. E. *J Controlled Release* 2004, 96, 37–53.
- 42 Rameez, S.; Alost, H.; Palmer, A. F. *Bioconjugate Chem* 2008, 19, 1025–1032.
- 43 Pang, Z. Q.; Lu, W.; Gao, H. L.; Hu, K. L.; Chen, J.; Zhang, C. L.; Gao, X. L.; Jiang, X. G.; Zhu, C. Q. *J Controlled Release* 2008, 128, 120–127.
- 44 Katz, J. S.; Zhong, S.; Ricart, B. G.; Pochan, D. J.; Hammer, D. A.; Burdick, J. A. *J Am Chem Soc* 2010, 132, 3654–3655.
- 45 Ghoroghchian, P. P.; Li, G. Z.; Levine, D. H.; Davis, K. P.; Bates, F. S.; Hammer, D. A.; Therien, M. J. *Macromolecules* 2006, 39, 1673–1675.
- 46 Sachl, R.; Uchman, M.; Matejcek, P.; Prochazka, K.; Stepanek, M.; Spirkova, M. *Langmuir* 2007, 23, 3395–3400.
- 47 Johnston, A. H.; Dalton, P. D.; Newman, T. A. *J Nanopart Res* 2010, 12, 1997–2001.
- 48 Labet, M.; Thielemans, W. *Chem Soc Rev* 2009, 38, 3484–3504.
- 49 Oshimura, M.; Takasu, A. *Macromolecules* 2010, 43, 2283–2290.
- 50 Chang, K. Y.; Lee, Y. D. *Acta Biomater* 2009, 5, 1075–1081.
- 51 Wang, G. W.; Huang, J. L. *J Polym Sci Part A: Polym Chem* 2008, 46, 1136–1150.
- 52 Xu, X. W.; Huang, J. L. *J Polym Sci Part A: Polym Chem* 2006, 44, 467–476.
- 53 Canaria, C. A.; Smith, J. O.; Yu, C. J.; Fraser, S. E.; Lansford, R. *Tetrahedron Lett* 2005, 46, 4813–4816.

- 54** Uyeda, H. T.; Medintz, I. L.; Jaiswal, J. K.; Simon, S. M.; Mattoussi, H. *J Am Chem Soc* 2005, 127, 3870–3878.
- 55** Bouzide, A.; Sauve, G. *Org Lett* 2002, 4, 2329–2332.
- 56** Petersen, M. A.; Yin, L. G.; Kokkoli, E.; Hillmyer, M. A. *Polym Chem* 2010, 1, 1281–1290.
- 57** Raynaud, J.; Absalon, C.; Gnanou, Y.; Taton, D. *J Am Chem Soc* 2009, 131, 3201–3209.
- 58** Luo, L. B.; Tam, J.; Maysinger, D.; Eisenberg, A. *Bioconjugate Chem* 2002, 13, 1259–1265.
- 59** Vangeyte, P.; Gautier, S.; Jerome, R. *Colloids Surf A* 2004, 242, 203–211.
- 60** Vangeyte, P.; Leyh, B.; Heinrich, M.; Grandjean, J.; Bourgaux, C.; Jerome, R. *Langmuir* 2004, 20, 8442–8451.
- 61** Zupancich, J. A.; Bates, F. S.; Hillmyer, M. A. *Macromolecules* 2006, 39, 4286–4288.
- 62** Liu, J. B.; Zeng, F. Q.; Allen, C. *Eur J Pharm Biopharm* 2007, 65, 309–319.
- 63** Gazeau-Bureau, S.; Delcroix, D.; Martin-Vaca, B.; Bonrissou, D.; Navarro, C.; Magnet, S. *Macromolecules* 2008, 41, 3782–3784.
- 64** Martin, A. L.; Bernas, L. M.; Rutt, B. K.; Foster, P. J.; Gillies, E. R. *Bioconjugate Chem* 2008, 19, 2375–2384.
- 65** Josephson, L.; Tung, C. H.; Moore, A.; Weissleder, R. *Bioconjugate Chem* 1999, 10, 186–191.
- 66** Lewin, M.; Carlesso, N.; Tung, C. H.; Tang, X. W.; Cory, D.; Scadden, D. T.; Weissleder, R. *Nat Biotechnol* 2000, 18, 410–414.
- 67** Nguyen, T.; Francis, M. B. *Org Lett* 2003, 5, 3245–3248.
- 68** Wu, P.; Malkoch, M.; Hunt, J. N.; Vestberg, R.; Kaltgrad, E.; Finn, M. G.; Fokin, V. V.; Sharpless, K. B.; Hawker, C. J. *Chem Commun* 2005, 5775–5777.
- 69** Chou, T. C.; Lin, K. C.; Wu, C. A. *Tetrahedron* 2009, 65, 10243–10257.
- 70** Peng, S. M.; Chen, Y.; Hua, C.; Dong, C. M. *Macromolecules* 2009, 42, 104–113.
- 71** Hua, C.; Peng, S. M.; Dong, C. M. *Macromolecules* 2008, 41, 6686–6695.
- 72** Gillies, E. R.; Jonsson, T. B.; Fréchet, J. M. J. *J Am Chem Soc* 2004, 126, 11936–11943.